DEUTSCHES ELEKTRONEN-SYNCHROTRON DESY

DESY 76/19
April 1976

受入
76-6-8
高工研図書室

Measurements of Dose and Shielding Parameters of Electron-Photon Stray Radiation from a High-Energy Electron Beam

by

H. Dinter and K. Tesch

2 HAMBURG 52 · NOTKESTIEG 1

To be sure that your preprints are promptly included in the
HIGH ENERGY PHYSICS INDEX ,
send them to the following address (if possible by air mail) :

DESY
Bibliothek
2 Hamburg 52
Notkestieg 1
Germany

Measurements of dose and shielding parameters of electron-photon stray radiation from a high-energy electron beam

by

H. Dinter and K. Tesch

Deutsches Elektronen-Synchrotron DESY, Hamburg

Summary:

The doses due to electron-photon stray radiation from an electron beam between 3 and 7 GeV are measured around iron targets. Shielding parameters are determined for several target geometries and for 5 shielding materials.

1. Introduction

For the design of the shielding of high-energy electron accelerators and their experimental facilities several radiation components have to be considered. The main radiation component from the interaction of the primary beam with some target material consists of photons and electrons of the electromagnetic cascade. The giant-resonance neutrons of low energies photoproduced within the cascade represent a second component. Neutrons with higher energies resulting from various other production processes have decreasing attenuation coefficients. Their intensity, however, also decreases rapidly above 100 MeV and so it is reasonable to define a high-energy neutron component between 50 and 100 MeV. The muons represent a forth component.

The dose caused by the muon component behind any shielding can be described by a mathematical expression since all cross sections and other data are well known. Nelson (ref. 1) has shown that his calculations agree with the experimental results with an accuracy being sufficient for radiation protection purposes. The production rates of the neutron components as a function of electron energy and of the angle of observation as well as their attenuation coefficients may either be taken from some experiments (see e.g. ref. 2-5) or approximately calculated (see e.g. ref. 6). In all these cases it is assumed that the primary beam is completely absorbed in a thick target. Otherwise the calculated dose can be reduced according to the fraction of the absorbed primary energy, since in most cases the self-absorption of the neutrons or muons in the target may be neglected, and since the production rate does not depend on the shape of the target.

There are also various experimental and theoretical investigations of the electron-photon component produced in a thick totally absorbing target (see e.g. ref. 2 and 7-9). Unfortunately the thick target geometry does not represent the real situation in shielding problems in most cases. More important and more realistic are situations where an electron beam

impinges on the thin sheet of a vacuum pipe at a small angle or strikes the edge of a magnet or of a collimator. The energy spectrum of the secondary electrons and photons extend to very low energies. Therefore the dose of this component at a given distance and for a given angle of observation strongly depends on the angle of incidence and on the shape of the target, and it is difficult to deduce it from the data of the electromagnetic cascade. The investigations of cascades are therefore of minor interest to the problem of shielding stray radiation.

Until now the dose resulting from electron-photon stray radiation produced at thin targets was measured only by Jenkins et al. (ref. 10) for some geometries. The absorption behaviour of this component was not studied. Usually it is assumed that the measured dose decreases exponentially with the minimum absorption coefficient, sometimes build-up factors are used.

In order to obtain more data on this component we measured the absorbed dose at a distance of 1 m for primary energies between 3 and 7.2 GeV. We used 14 simple target geometries which easily may be adapted to realistic situations. In addition the attenuation parameters for the five most important shielding materials were determined.

2. Experimental Set-up

The measurements were performed on an electron beam of an average intensity of 2 10^{10} s^{-1} and of a diameter of 1 cm at the target. The intensity was measured by a secondary-emission monitor placed in front of the target; the monitor could be calibrated by means of a Faraday-cup. Iron targets of various thicknesses were positioned at different angles with respect to the beam (see the notations in fig. 1).

For 14 combinations of angle and thickness d, the dose of the electron-photon stray radiation was measured at 20 angles of observations θ and at energies of 3 GeV, 5 GeV and 7.2 GeV. For the dose measurements we used thermoluminescence dosemeters consisting of ^{7}LiF whose sensitivity against neutrons may be neglected. Their dimensions were 3.2 3.2 0.9 mm^3 for low doses and 6.01 mm 1.0 mm dia. for higher doses. They were located in small plastic boxes with a wall thickness of 1 mm. Measurements showed that thicknesses of more than 1 mm already reduced the doses. The dosemeters are calibrated in units of absorbed dose (rad) by means of ^{60}Co -rays.

The experimental set-up was placed inside a shielding house made of concrete so that the walls were at a distance of 1.7 to 3 m from the target. Therefore we expected a noticeable background in the dose measurements at 1 m distance. However we found in the region θ 30°, where the angular distribution is rather flat, a $1/r^2$-dependence within an error of 20%. So we added no further correction. Since all other errors are smaller, we obtained an accuracy of 20% for the dose measurements.

The shielding parameters for the five most important shielding materials (lead, iron, heavy concrete, ordinary concrete and sand) were determined at 7 GeV for the target geometries mentioned above. We used absorber plates of 40 40 cm^2 size. The dosemeters were positioned in the middle of each gap between the plates. The whole stack was surrounded by 5 cm iron and 20 cm lead except at the front side. Iron was used in order to

reduce backscattering. A maximum of 60 cm was possible for the total stack thickness. For greater depths in the case of concrete and sand, solid blocks (without dosemeters) were placed in front of the stack. The whole set-up could be positioned at $\theta = 90^{o}$ and at $\theta = 30^{o}$.

The attenuation coefficients are usually defined for an unshielded detector at a constant distance from the radiation source and for an absorber with large lateral dimensions between source and detector. Our set-up differs from this ideal arrangement in some respects. The stack of plates permits us to measure the attenuation of a whole series of shielding walls in one run. However, the resulting attenuation coefficients may differ from those determined by an unshielded detector due to the backscattering of the plates behind it. Experiments showed that backscattering is only noticeable in the case of lead absorbers and for the first unshielded dosemeter in front of the iron plates. For lead, the backscattering contributes roughly 25% of the dose rather independent of the absorber depth; for the front dosemeter it amounts to 50%. We conclude that our measurements using a stack of plates yield the correct attenuation coefficients if, in addition, corrections are made for the varying distance. Since the distance between the target and the detectors varies between 1.5 m and 2.1 m these corrections (assuming a $1/r^2$ dependence) are small. Several checks with a fixed detector and a variable absorber thickness showed that these considerations hold even for the lead stack.

Other shortcomings are the small size of the plates and the limited range of depths. Yet the size of our detectors is very small, and for greater thicknesses the measured attenuation curves bend into a slope determined by the minimum-attenuation coefficient for each material. In the case of ordinary concrete our values agree approximately with those of Kirn and Kennedy who used plates of $2.5 \cdot 2.5\ m^2$ size (see chapter 3). From these facts we conclude that our shielding parameters also apply to large absorber walls and that the measured curves can be continued to even greater depths.

3. Results

3.1 Dose data

The measured doses $D_T(\theta)$ at a distance of 1 m from the target for $1 \cdot 10^{11}$ primary electrons of 5 GeV energy are shown in figs. 2 - 5 as a function of the angle θ. The strong dependence on the target geometry is obvious. The dip at small negative angles is due to the self-absorption in the target when the angle θ coincides with the target angle φ . For an effective target thickness $d/\sin\varphi < 15$ cm the exit point of the beam is the most intense source, otherwise the scattered radiation from the entrance point is the dominating one. For shielding design those data from figs. 2 - 5 may be taken as source data, which will describe the actual situation in the best way.

The measurements can be compared only indirectly with the data from Jenkins et al. (ref. 10). If the SLAC data for the scattering from a thin aluminium plate are adapted to our situation by using the appropriate radiation lengths and effective target thicknesses, their dose curve should lie between our curves for $\varphi = -5^\circ$ and $\varphi = -12^\circ$ in fig. 2, which is actually the case.

The dependence of the doses on the primary energy also varies with the target geometry. Energy independence is expected for thin targets and proportionality for thick targets. Our measurements between 3 and 7.2 GeV give results independent of energy for d = 0.2 cm and $d/\sin\varphi < 2$ cm. For $d/\sin\varphi > 8$ cm we see a linear increase with energy. A linear increase is also obtained for thick targets (> 1 cm), if the detector is on the same target side as the beam exit point; otherwise the doses increase proportionally to $\sqrt{E}$.

3.2 Shielding parameters

In figs. 6 and 7 attenuation curves are shown for an iron target with d = 0.2 cm and $\varphi = +2^\circ$ and for a primary electron energy of 7 GeV. It is

remarkable that in this case approximately 99% of the dose $D_T(\theta)$ given in section 3.1 is due to very low energy radiation. If these doses are used as source data in shielding calculations, the usual exponential decrease of the intensity should not be applied. Instead we assume the following dependence of the dose $D(\theta, x)$ on the shielding thickness x for a given primary electron beam:

$$D(\theta, x) = D_T(\theta)\, A_T\, e^{-\lambda x} \quad \text{for } x > x_A.$$

In this way the absorption of the low-energy component in the very first part of the shield ($x < x_A$) is accounted for by the absorption factor A_T, which depends on the target geometry.

We measured the parameters A_T, λ and x_A for several target geometries. As expected the values for λ and x_A are independent of the target arrangement; they are indicated in tab. 1 and 2. The values are in good agreement with the minimum absorption coefficients. The error in the "recommended values" is roughly 3% for lead and iron and 7% for the concretes and for sand.

The values A_T strongly depend on the target geometry. They are listed in tab. 3. In addition mean values are given to facilitate the use of these data.

Some measurements were performed (near $\theta = 90^\circ$) to study the composition of the low-energy component. We used thin absorbers made of aluminium, iron and lead in connection with a permanent-magnet arrangement preventing electrons below 300 MeV from reaching the dosemeters. The results can be summarized as follows: at absorber depths smaller than 5 g/cm^2 the dose is caused by electrons below 10 MeV multiply scattered into large angles and by photons around 0.1 MeV from the Compton scattering of low-energy bremsstrahlung. The ratio between the two components is roughly 3 : 1. In the range 10 to 30 g/cm^2 the dose is due to photons around 0.3 to 0.5 MeV from Compton scattering and positron-electron annihilation. At greater depths the dose is determined by photons of

energies corresponding to the minimum absorption coefficient.

These results on the composition of the low-energy stray radiation are supported by Monte-Carlo calculations performed with the code EGS (ref. 12). A 7-GeV electron beam impinging on an iron target with d = 1 cm and $\varphi = -5^{o}$ was simulated. The low-energy part of the spectra of electrons and photons scattered at 90^{o} are shown in figs. 8 and 9. Clearly seen is the dominance of electrons with energies as low as a few MeV (the cut-off energy of the code is 1.5 MeV). The photon spectrum (fig. 8) is dominated by photons around 100 keV and by the annihilation radiation in qualitative agreement with our measurements.

Acknowledgement

The help of the Hallendienst group is greatfully acknowledged. We are especially grateful to Dr. F. Schwickert for his permanent efforts in supporting this experiment.

Literature

1. W. R. Nelson, Nucl. Instr. Meth. 66 (1968) 293, 120 (1974) 401 and 413
2. G. Bathow, E. Freytag and K. Tesch, Nucl. Phys. B 2 (1967) 669
3. G. Bathow, E. Freytag and K. Tesch, Nucl. Instr. Meth. 33 (1965) 261
4. J. J. Broerse and F. J. Van Werven, Health Physics 12 (1966) 83
5. L. N. Zaitsev et al., Atomnaya Energiya 19 (1965) 303, 20 (1966) 355, 20 (1966) 355, 12 (1962) 524
6. R. G. Alsmiller and J. Barish, Report ORNL-TM-4060 (1973)
7. G. Bathow, E. Freytag, M. Köbberling, R. Kajikawa and K. Tesch Nucl. Phys. B 20 (1970) 592
8. C. J. Crannel, Phys. Rev. 161 (1967) 310
9. U. Völkel, Report DESY 65/6 (1965), 67/16 (1967)
10. T. M. Jenkins, G. J. Warren and J. L. Harris, Report SLAC-TN-70-34 (1970)
11. F. S. Kirn and R. J. Kennedy, Nucleonics 12 (1954), 6, 44
12. The code EGS was kindly given at our disposal by R. L. Ford and W. R. Nelson, High-Energy Physics Laboratory and Stanford Linear Accelerator Center, Stanford.

Tab. 1 Attenuation coefficients λ (cm^{-1}) measured with several target arrangements (see fig. 1) and comparison with other values.

Shielding material	Density (g cm^{-3})	d = 0.2 cm; φ = -2^o ϑ = -90^o	ϑ = $+30^o$	d=10 cm φ=90^o ϑ=-90^o	Min. absorpt. coeff.	other measure ments	recommended value
Lead	11.3	0.47	0.46		0.47		0.47
Iron	7.8	0.23	0.23		0.23		0.23
Heavy concrete *)	3.7	0.086	0.085	0.089	0.093	0.065.. ..0.075 (Ref.3)	0.080
Ordinary concrete	2.4	0.056	0.061		0.048	0.050 (Ref.11)	0.055
Sand	1.3 **)	0.025			0.026		0.025

*) Fe 51%, O 34%. Si 7%, Ca 5%, Mg 2%, Al 1% by weight

**) In nature the density of sand is roughly 1.6 g cm^{-3}.

Tab. 2 Shielding thickness x_A (cm) absorbing the low energy component.

Material	x_A
Lead	2
Iron	6
Heavy concrete	20
Ordinary concrete	25
Sand	50

Tab. 3 Absorption factor A_T measured for several target arrangements (see fig. 1)

d (cm)	φ	A_T $\theta = +30^\circ$	A_T $\theta = +90^\circ$
0.2	- 1	0.053	0.0077
	- 5	0.036	0.012
	- 12	0.037	
	90		0.007
1	- 2	0.24	0.023
	- 5	0.11	0.013
	- 12	0.070	~ 0.01
	90	~ 0.09	
5	- 5	1.0	0.18
	+ 5	0.51	0.038
	+ 12	1.0	0.076
	- 12	0.61	0.10
	90	0.17	0.040
10	- 12	1.0	0.42
	+ 12	1.0	0.11
	90	0.24	0.027
		Mean values:	
0.2	$1^\circ \ldots 15^\circ$, 90°	0.05	0.009
1	$2^\circ \ldots 15^\circ$, 90°	0.1	0.02
5	$5^\circ \ldots 15^\circ$, 90°	0.8 0.2	0.1 0.03
10	12° 90°	1.0 0.2	0.3 0.03

Figure captions

Fig. 1 Symbols denoting the target geometry

Fig. 2-5 The dose D_T of the electron-photon stray radiation at a distance of 1 m from an iron target of thickness d and at an angle φ (see fig. 1), as a function of the angle of observation θ. Primary beam: $1 \cdot 10^{11}$ electrons, 5 GeV. The points are indicated by the symbols + and -, where the results for positive and negative values are different, otherwise they are marked by crosses.

Fig. 6-7 The attenuation of the electron-photon stray radiation by several absorbers at $\theta = -90^{\circ}$. The iron target has d = 0.2 cm and $\varphi = +2^{\circ}$ (see fig. 1), the distance from the target is 2 m. Primary beam: $1 \cdot 10^{11}$ electrons, 7.2 GeV.

Fig. 8 The calculated spectrum of low-energy electrons scattered from a thin iron target resulting from 300 primary electrons with an energy of 7 GeV.

Fig. 9 The calculated spectrum of low-energy photons scattered from a thin iron target resulting from 300 primary electrons with an energy of 7 GeV.

Fig. 1

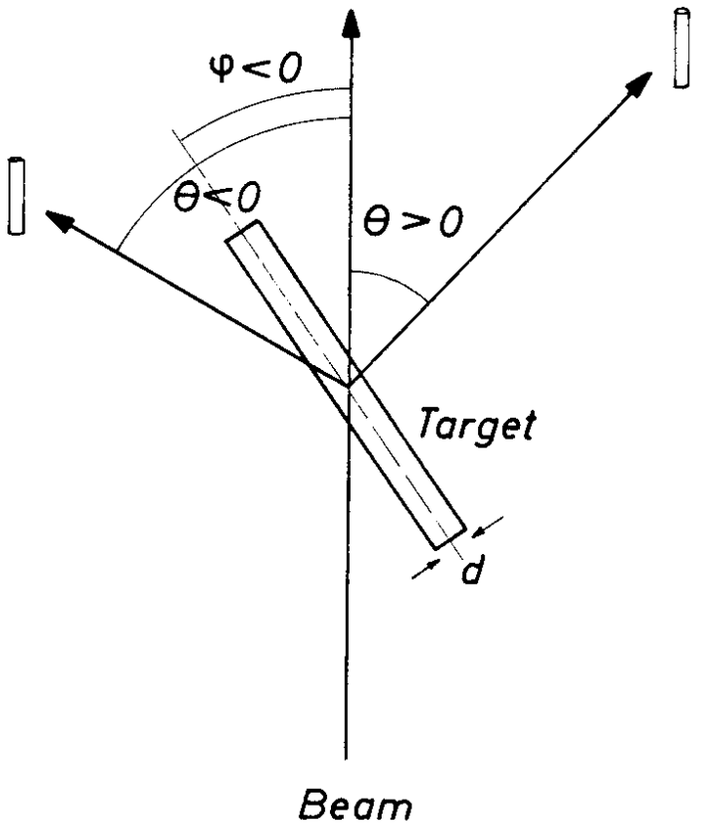

Fig. 2

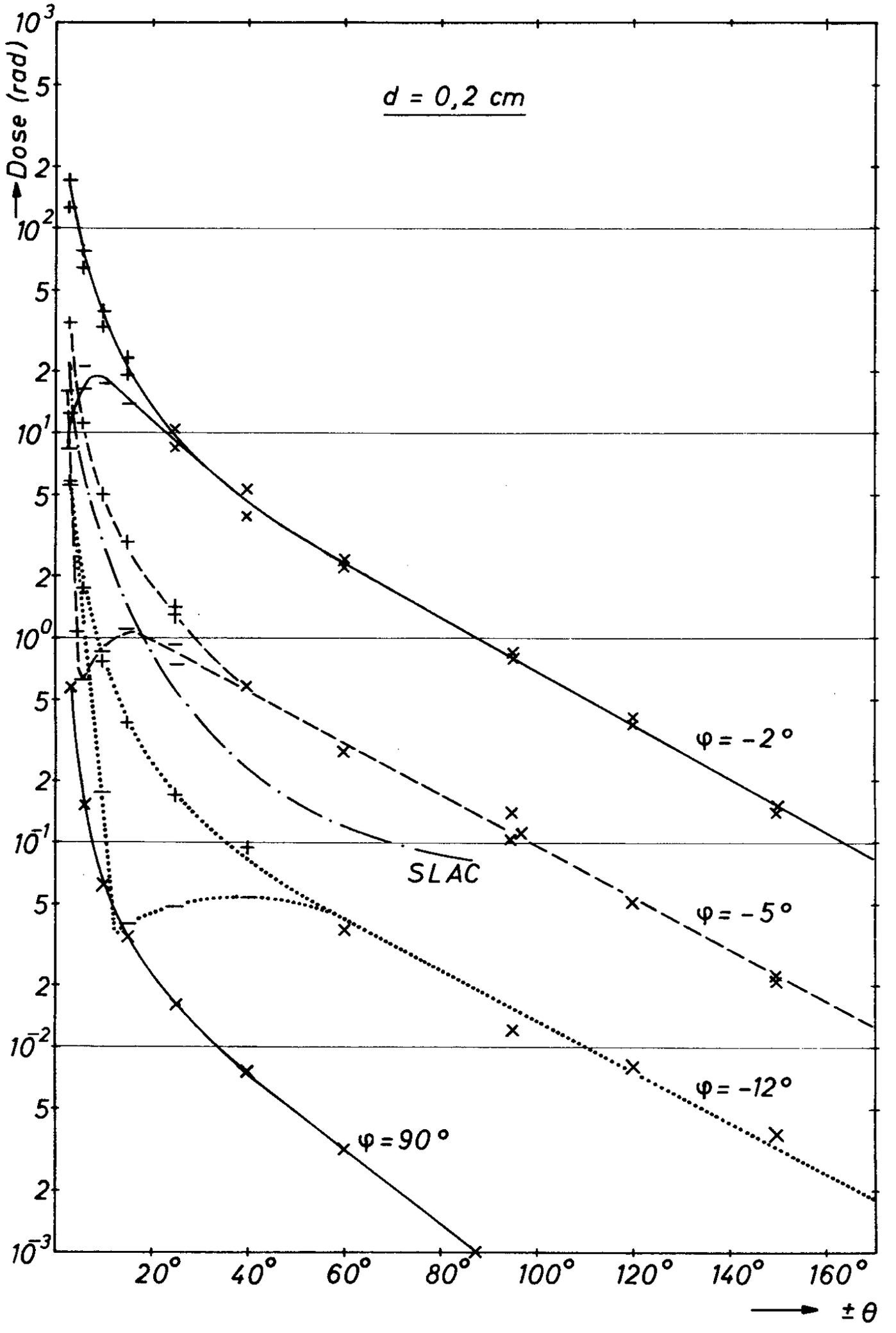
d = 0,2 cm
Dose (rad)
10^3
5
2
10^2
5
2
10^1
5
2
10^0
5
2
10^-1
5
2
10^-2
5
2
10^-3
φ = -2°
SLAC
φ = -5°
φ = -12°
φ = 90°
20°
40°
60°
80°
100°
120°
140°
160°
± θ

Fig. 3

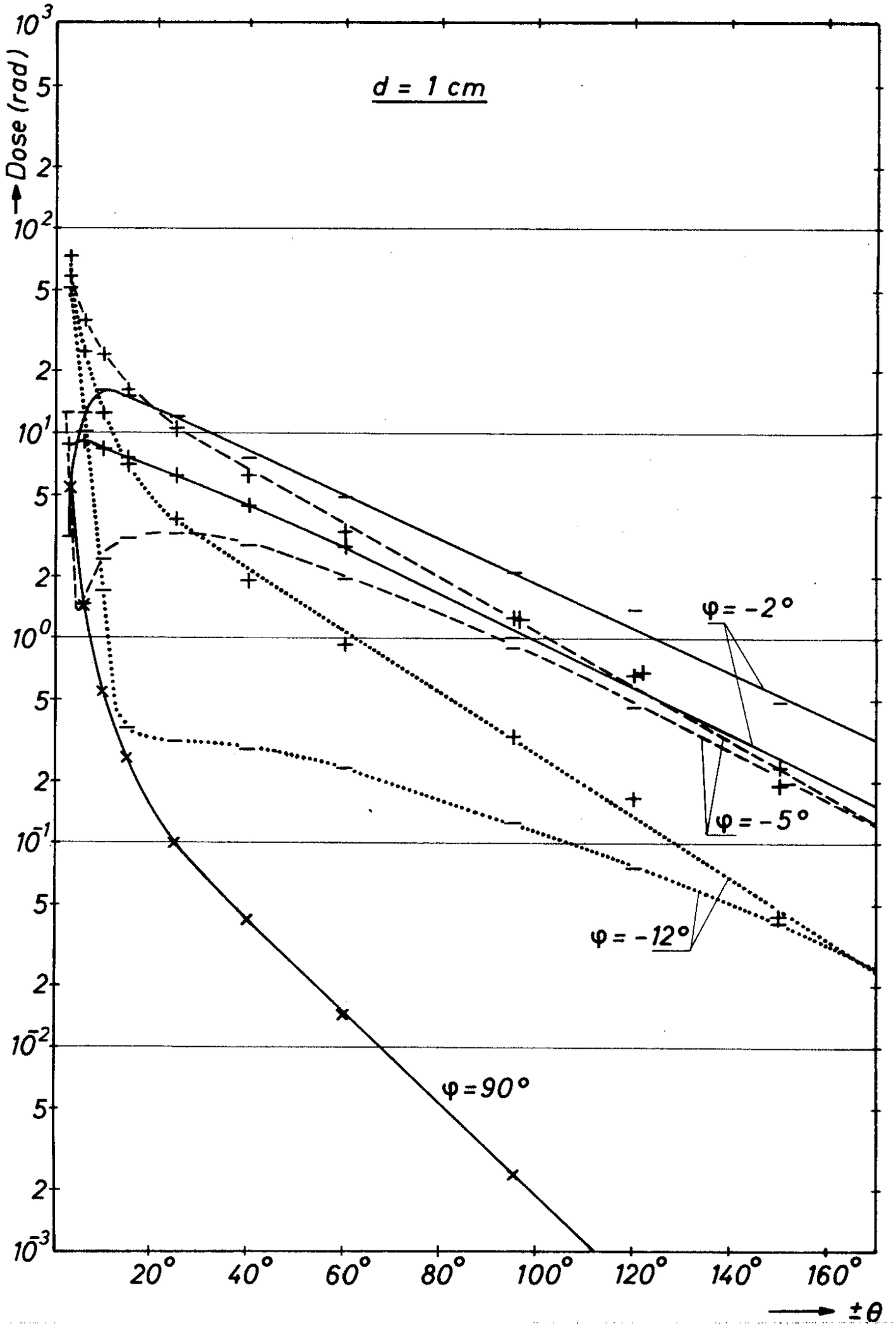
d = 1 cm
Dose (rad)
10^3
5
2
10^2
5
2
10^1
5
2
10^0
5
2
10^{-1}
5
2
10^{-2}
5
2
10^{-3}
φ = −2°
φ = −5°
φ = −12°
φ = 90°
20°
40°
60°
80°
100°
120°
140°
160°
± θ

Fig. 4

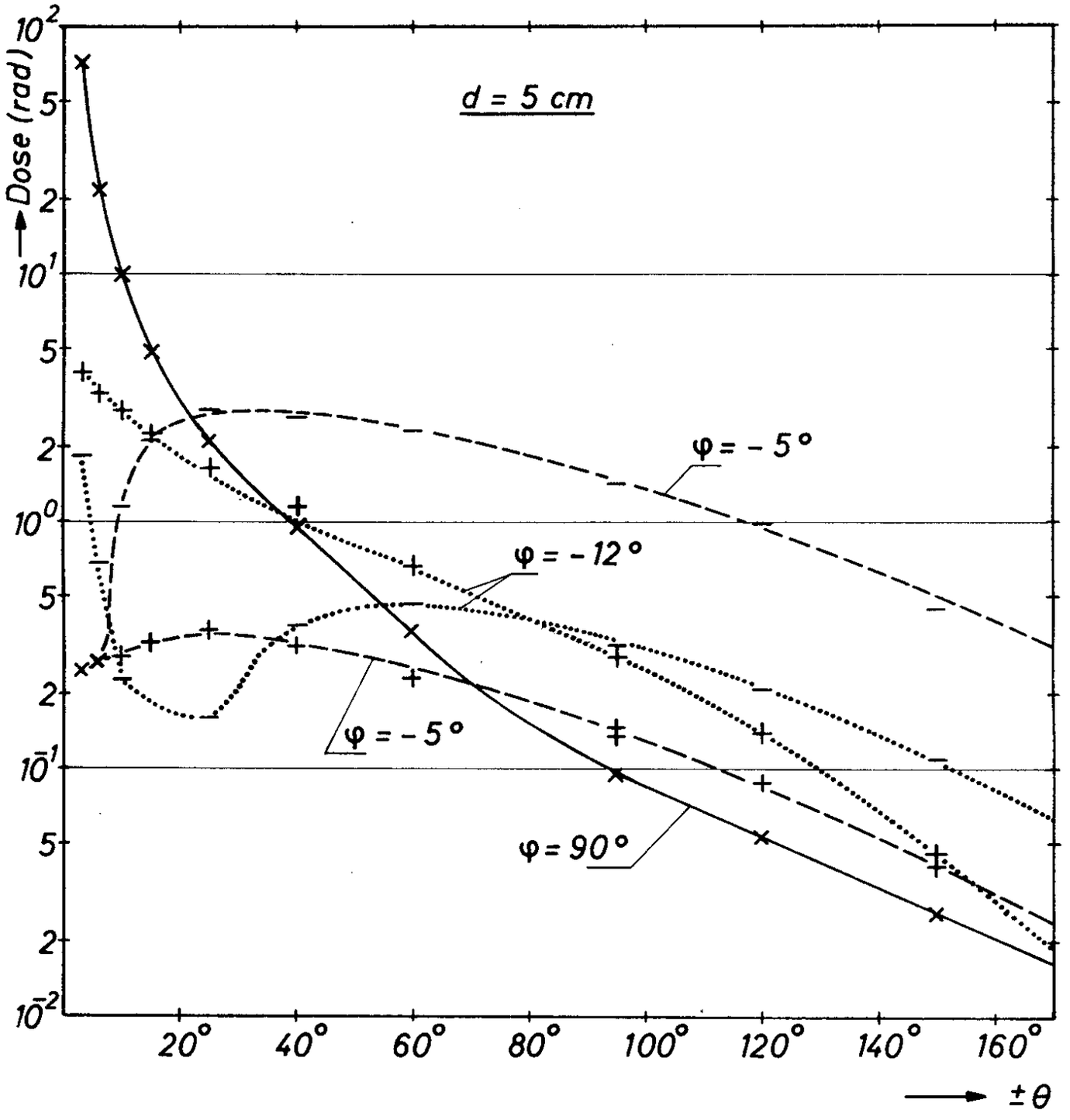
d = 5 cm
Dose (rad)
10^2
5
2
10^1
5
2
10^0
5
2
10^-1
5
2
10^-2
φ = - 5°
φ = - 12°
φ = - 5°
φ = 90°
20°
40°
60°
80°
100°
120°
140°
160°
± θ

Fig. 5

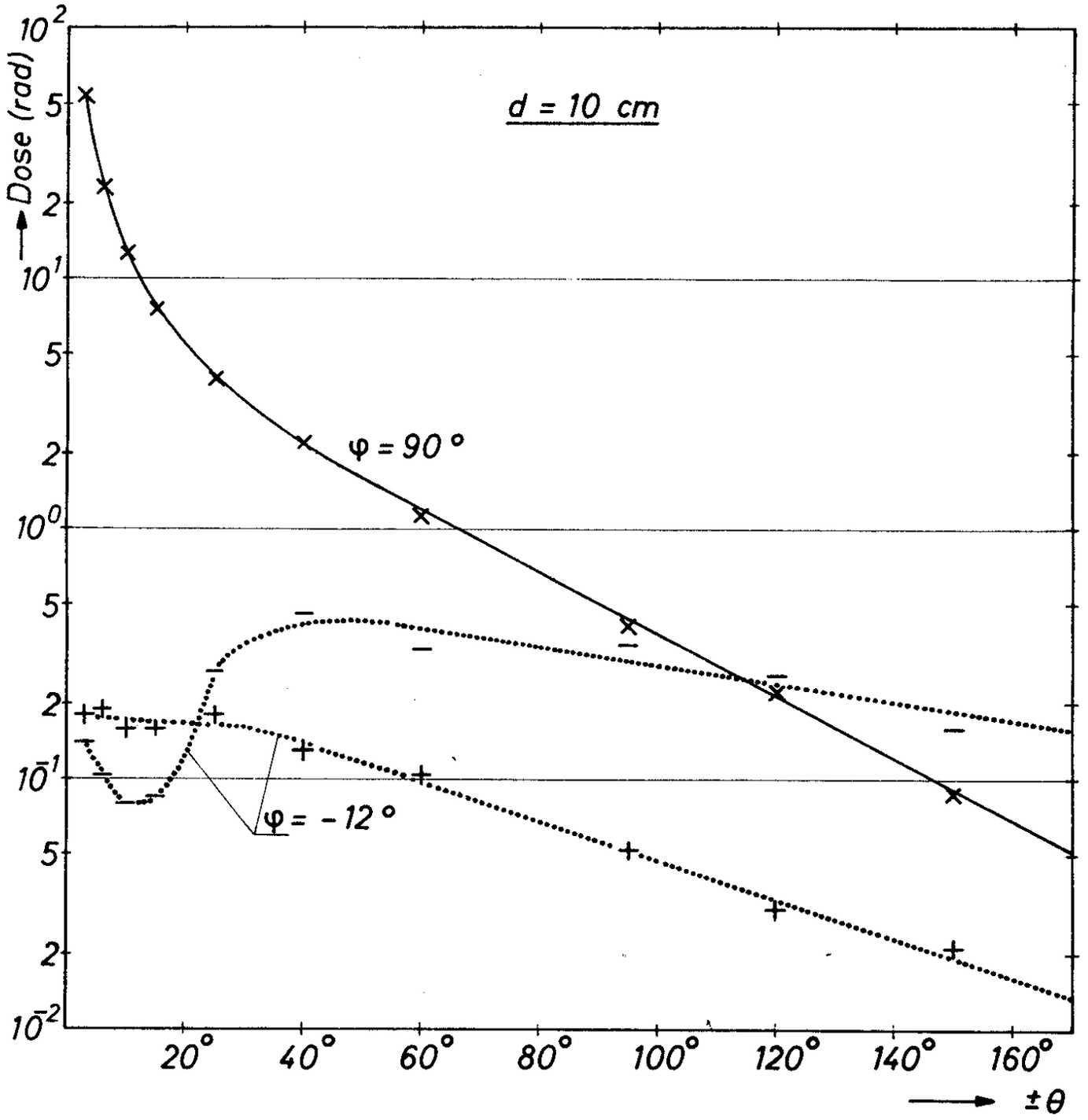
d = 10 cm
Dose (rad)
10^2
5
2
10^1
5
2
10^0
5
2
10^-1
5
2
10^-2
φ = 90°
φ = -12°
20°
40°
60°
80°
100°
120°
140°
160°
±θ

Fig. 6

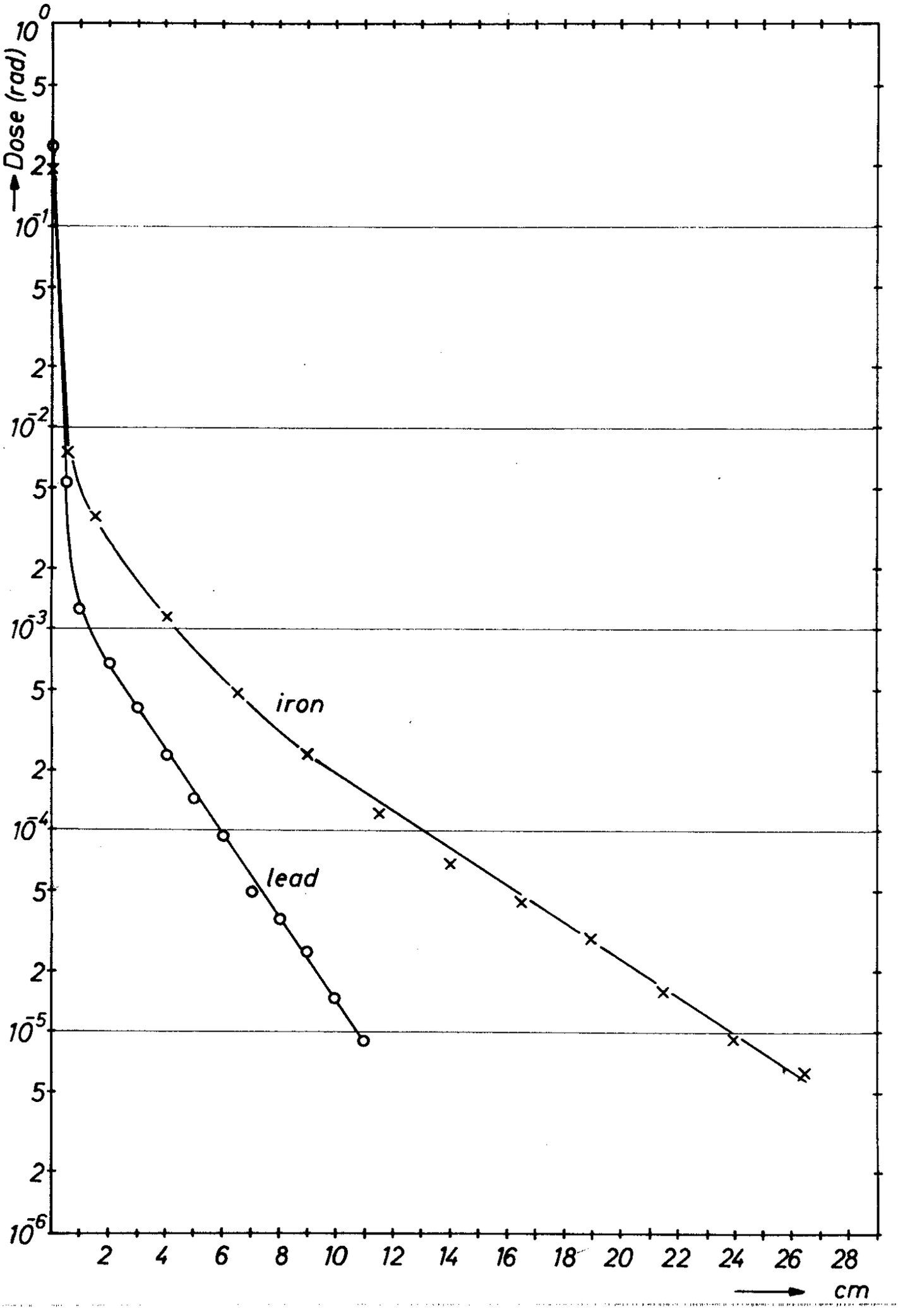
Dose (rad)
10^0
5
2
10^-1
5
2
10^-2
5
2
10^-3
5
2
10^-4
5
2
10^-5
5
2
10^-6
iron
lead
2
4
6
8
10
12
14
16
18
20
22
24
26
28
cm

Fig. 7

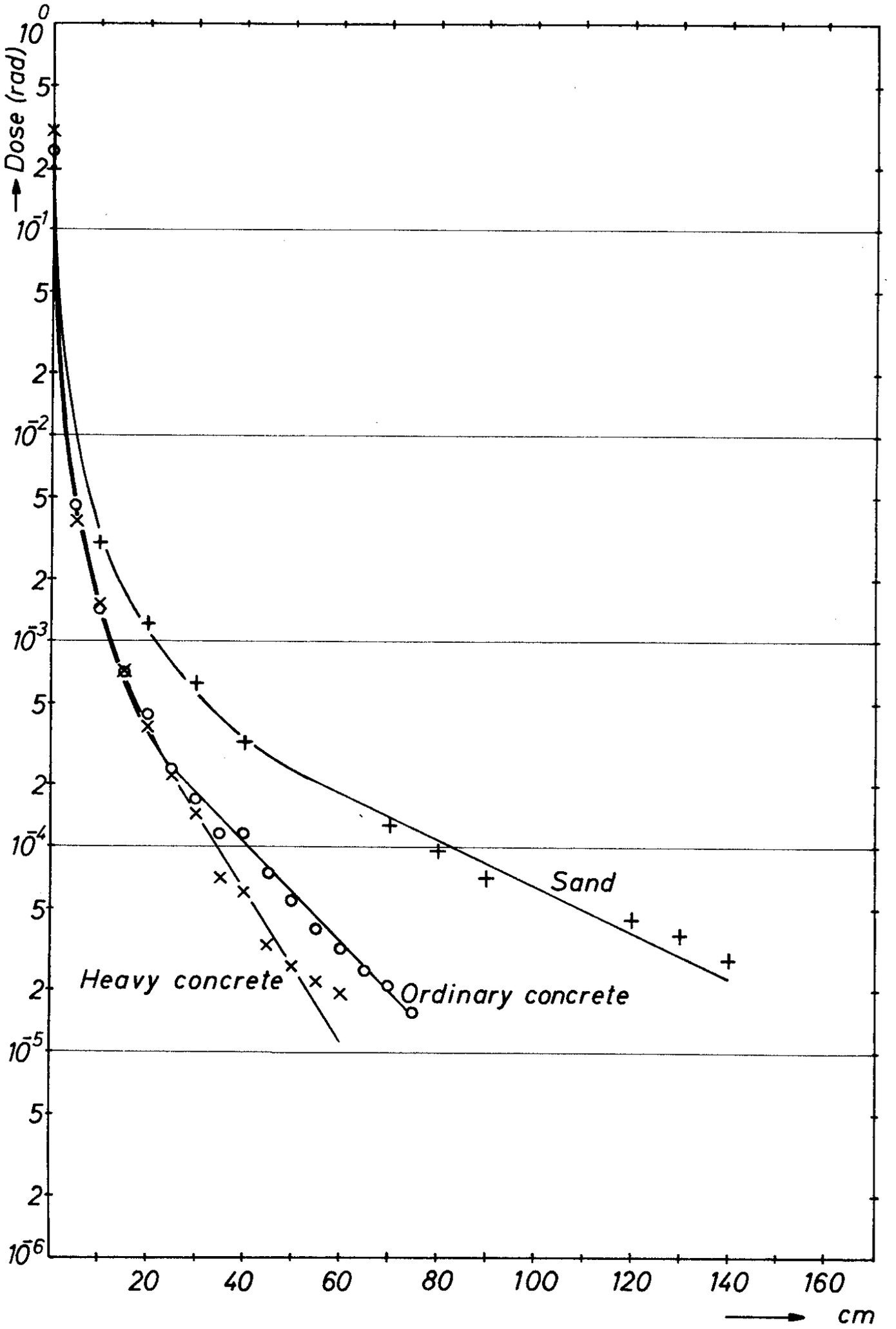
Dose (rad)
10^{0}
5
2
10^{-1}
5
2
10^{-2}
5
2
10^{-3}
5
2
10^{-4}
5
2
10^{-5}
5
2
10^{-6}
20
40
60
80
100
120
140
160
cm
Sand
Heavy concrete
Ordinary concrete

Fig. 8

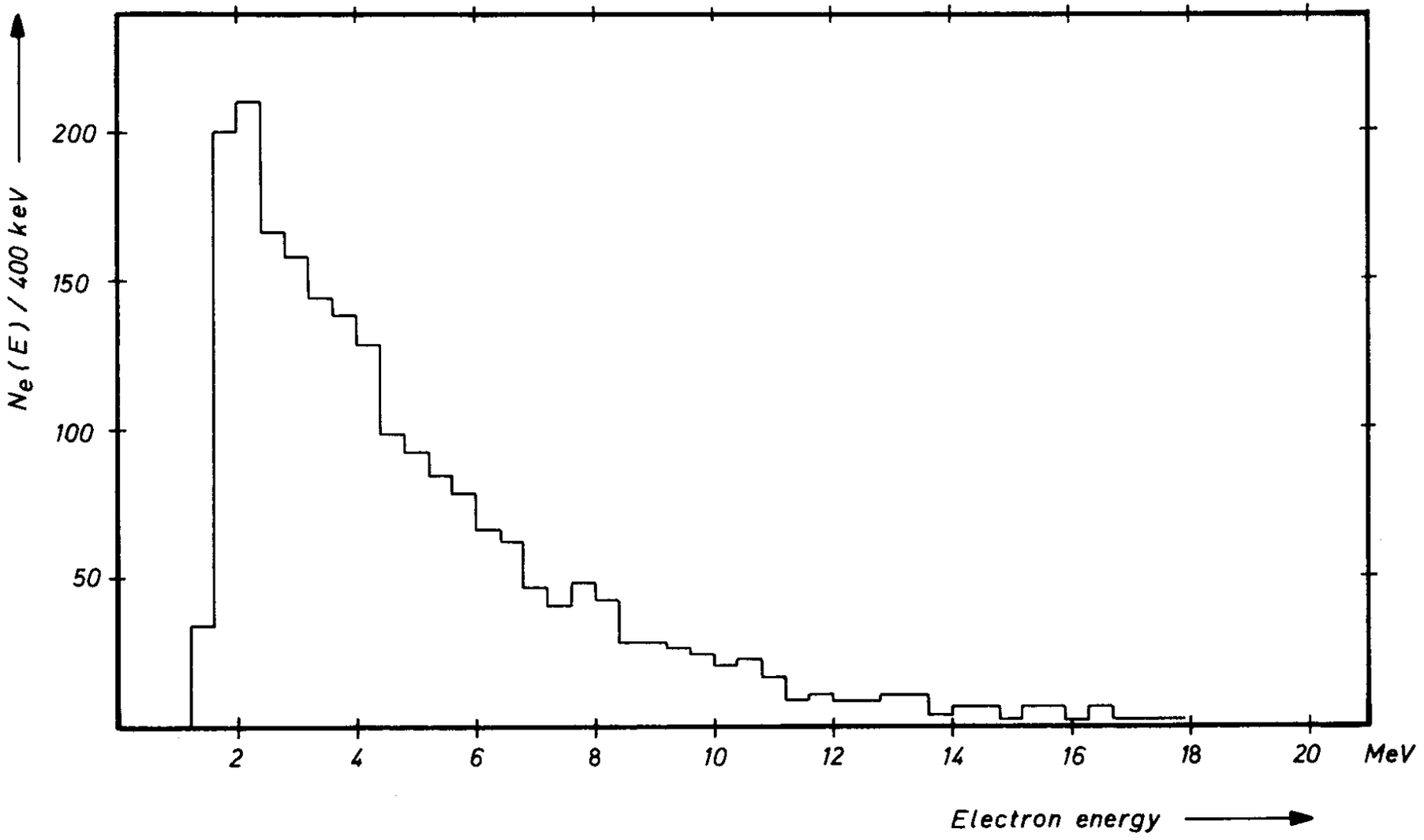
$N_e(E)$ / 400 keV
200
150
100
50
2
4
6
8
10
12
14
16
18
20
MeV
Electron energy

Fig. 9

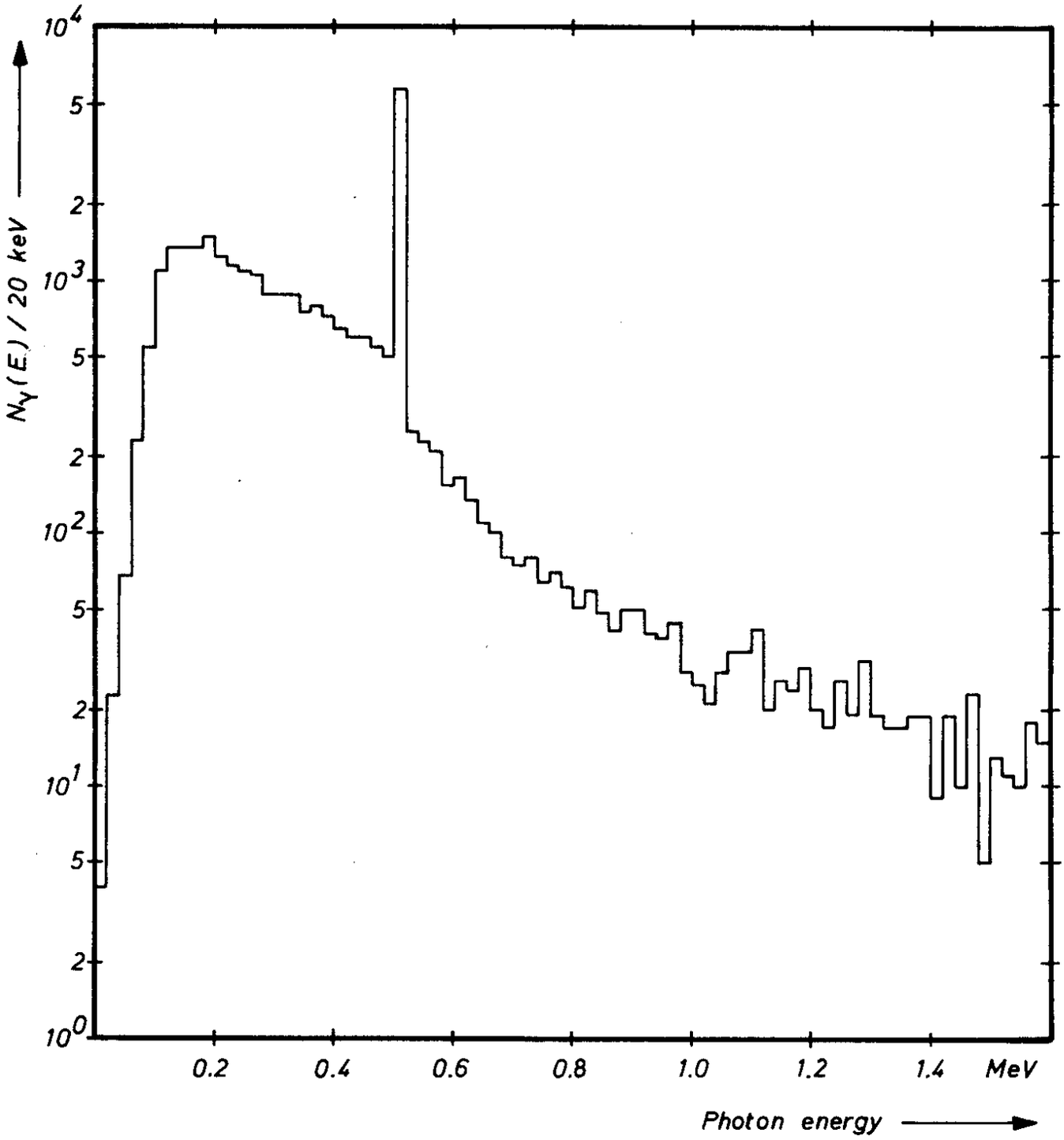
10^4
5
2
10^3
5
2
10^2
5
2
10^1
5
2
10^0
$N_\gamma(E_\gamma)$ / 20 keV
0.2
0.4
0.6
0.8
1.0
1.2
1.4
MeV
Photon energy